

Article

Stabilizing a Zn Anode by an Ionic Amphiphilic Copolymer Electrolyte Additive for Long-Life Aqueous Zn-Ion Batteries

Yu-E Liu and Xin Wang * 

Songshan Lake Materials Laboratory, Dongguan 523808, China

* Correspondence: wangxin@sslslab.org.cn

Abstract: The rampant growth of zinc dendrites and severe uncontrollable reactions have largely limited the industrialization of aqueous Zn-ion batteries. Electrolyte additive engineering was found to be a facile yet effective strategy in addressing these issues; however, traditional organic small molecule additives raise additional safety and health risks and thus compromise the intrinsic advantage of aqueous batteries. In this study, we report a polyacrylonitrile-*co*-poly(2-acrylamido-2-methylpropanesulfonic acid) (PAN-*co*-PAMPS) copolymer with ionic and hydrophilicity PAMPS and non-ionic PAN, which acts as an electrolyte additive to regulate the Zn deposition in aqueous Zn-ion batteries. The hydrophilicity of PAMPS is designed to meet water solubility. Moreover, ionic PAMPS reacts with a Zn anode surface, chemically peels the surface, leaves a pre-polished anode surface, and removes heterogeneity and impurity of the metal surface. All these effects are beneficial for homogeneous zinc ion deposition and long-life battery. The PAN segments act as a water-shielding layer on a Zn anode to prevent its direct contact with H₂O. Consequently, the Zn|Zn symmetric cells with additive-containing electrolytes have a much longer life than those without additives (up to eight times) at a current density of 1 mA cm⁻² and a capacity of 1 mA h cm⁻². The assembled Zn|Cu cells and the Zn|V₂O₅ full batteries also display prominent electrochemical reversibility. The reactively acidic amphiphilic polymer provides not only an alternative strategy for the design of multi-functional electrolyte additives, but also constitutes an easy-to-operate way for advancing commercialization of aqueous zinc-storage devices.

Keywords: aqueous batteries; Zn-based energy storage; electrolyte additive; ionic amphiphilic copolymer



Citation: Liu, Y.-E.; Wang, X.

Stabilizing a Zn Anode by an Ionic Amphiphilic Copolymer Electrolyte Additive for Long-Life Aqueous Zn-Ion Batteries. *Batteries* **2023**, *9*, 25. <https://doi.org/10.3390/batteries9010025>

Academic Editor: Carlos Ziebert

Received: 30 October 2022

Revised: 10 December 2022

Accepted: 15 December 2022

Published: 29 December 2022



Copyright: © 2022 by the authors. Licensee MDPI, Basel, Switzerland. This article is an open access article distributed under the terms and conditions of the Creative Commons Attribution (CC BY) license (<https://creativecommons.org/licenses/by/4.0/>).

1. Introduction

Aqueous Zn-ion batteries (AZIBs) have emerged as next-generation grid-scale energy storage devices with the increasing demand of global carbon neutrality. AZIBs stand out among other rechargeable batteries for energy storage because an aqueous electrolyte is extremely high in safety, in addition to the highly abundant Zn resources on earth. AZIBs employing a Zn metal anode have a large theoretical capacity of 820 mA h g⁻¹, which is much higher than other energy storage counterparts [1–5]. However, the uneven deposition and nucleation of Zn²⁺, and the interfacial side reactions cause uncontrollable growth of the Zn dendrite during the cycling of battery, resulting in lower Coulombic efficiency (CE) and compromising cycling lifespans that limit their commercialization [6,7]. Numerous efforts have been dedicated to address these issues and have achieved great results, including anode surface/interface construction and modification, electrode/host structure design, electrolyte engineering, and separator optimization [8–14]. Electrolyte additive engineering that involves the introduction of trace functional moieties either in the form of a small molecule or macromolecule may be the most convenient and cost-effective strategy. Therefore, electrolyte additive engineering has always been the first choice to stabilize Zn anodes in attempts toward creating long-life batteries [15–19].

In the endeavor of exploring suitable electrolyte additives for AZIBs, polar organic solvents that preferentially associate with H₂O have been primarily selected. For example,

adding dimethyl sulfoxide (DMSO) into 2 M ZnSO_4 was found to largely inhibit side reactions and dendrites [20–23]. Other small molecules, such as the organic acetonitrile [24–26], ethylene glycol [27], trimethyl phosphate [28,29], and dioxane [30], as well as inorganic graphene oxide (GO) [31], were also added to conventional aqueous electrolytes to show the suppression on Zn dendrites. However, organic solvents and small molecules cause some safety and health risks, so they are less desirable for aqueous batteries. Other researchers increased the concentration of electrolytes to reduce the activity of H_2O for longer cycle lives [32,33], yet the additional cost of extra electrolyte needs to be controlled to an industrialization level. The first and the most common role of an electrolyte additive is to desolvate the Zn^{2+} to reduce the number of solvated H_2O on the metal salt [34,35]. This generally decreases the activity of H_2O and allows for faster ion transportation and suppresses the water-related side reaction in the bulk electrolyte solution. Hydrophilic polymers are potentially good additives for AZIBs because of their excellent solubility and nontoxicity. With proper modification of the polymer chain, such as copolymerizing, a comonomer of different hydrophilicity, hydrophilic polymers can be added to aqueous electrolytes to adjust the solvation structure and uniform deposition of zinc ions, with synergistic effect if the polymers have a multiphase structure [36].

Herein, a polyacrylonitrile-*co*-poly(2-acrylamido-2-methylpropanesulfonic acid) (PAN-*co*-PAMPS) copolymer with hydrophobic PAN and acidic reactive PAMPS segments was first introduced to AZIBs to regulate the zinc deposition in cycling. The sulfonic acid PAMPS is an ionic polyelectrolyte in water with higher ionic conductivity than other polymers because of its sulfonic acid group [37]. The acidity of PAMPS can chemically polish a Zn anode to remove heterogeneity while providing adequate water solubility for the copolymer. On the other hand, the hydrophobic PAN segments act as a water-shielding layer on a Zn anode to prevent its direct contact with H_2O . The schematic illustration of the functional mechanism of PAN-*co*-PAMPS is shown in Figure 1. The characterization results show that the hydrophilicity of the electrolyte increases after addition of the amphiphilic copolymer additive. PAMPS segments peel the surface of the Zn anode, and PAN segments prevent the Zn anode from contact with H_2O directly. All these contributions facilitate the even nucleation and deposition of Zn^{2+} , thus increasing the cycling lifespan and overall electrochemical performance of AZIBs. The Zn|Zn symmetric cell with stable PAN-*co*-PAMPS additive cycles over 2400 h at a current density of 2 mA cm^{-2} is shown. The Zn|Cu asymmetric cells and the Zn| V_2O_5 full batteries assembled with the PAN-*co*-PAMPS additive also display prominent electrochemical reversibility compared to those without the additive.

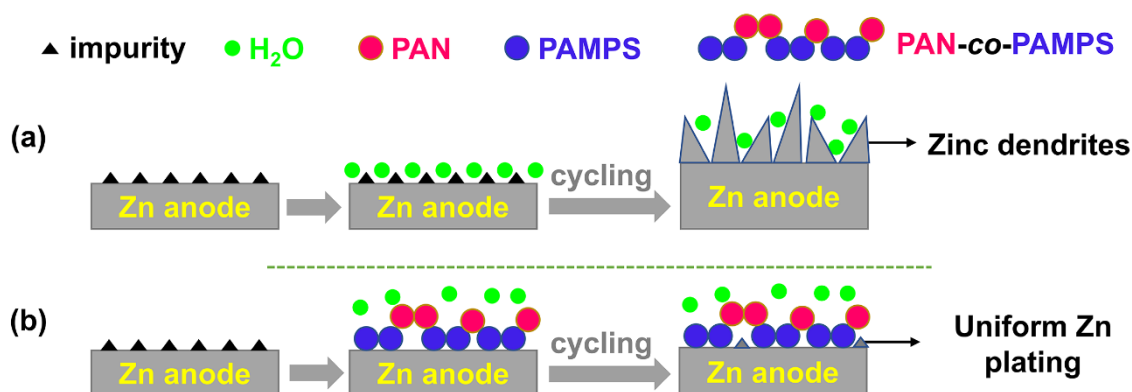


Figure 1. Schematic illustration of the Zn-stabilizing mechanism of PAN-*co*-PAMPS. Molecule distribution at the surface of Zn anode of Zn|Zn symmetric cell using (a) pristine and (b) additive-containing electrolyte.

2. Results and Discussion

Figure 2a shows that the prepared PAN-*co*-PAMPS has only one glass transition temperature at 87 °C, indicating that this is a random copolymer rather than a mixture or block copolymer. The glass transition temperature was found to be lower than that of homo-PAN at 96 °C, which further indicated that the copolymer was successfully synthesized. The FTIR spectrum in Figure S1 and ¹H NMR spectrum in Figure S2 further indicates that the target copolymer has been successfully synthesized containing 30 mol.% of AN segment. Table S1 shows the molecular weight of PAN-*co*-PAMPS with a number-molecular weight (*M_n*) of about 42k and a weight-molecular weight (*M_w*) of about 165k. The content of additive, 0.5 wt.%, is confirmed by the solubility of the additive in the electrolyte and the cycle life of the Zn | Zn symmetric cell at a current density of 5 mA cm⁻², as shown in Supplementary Figures S3 and S4.

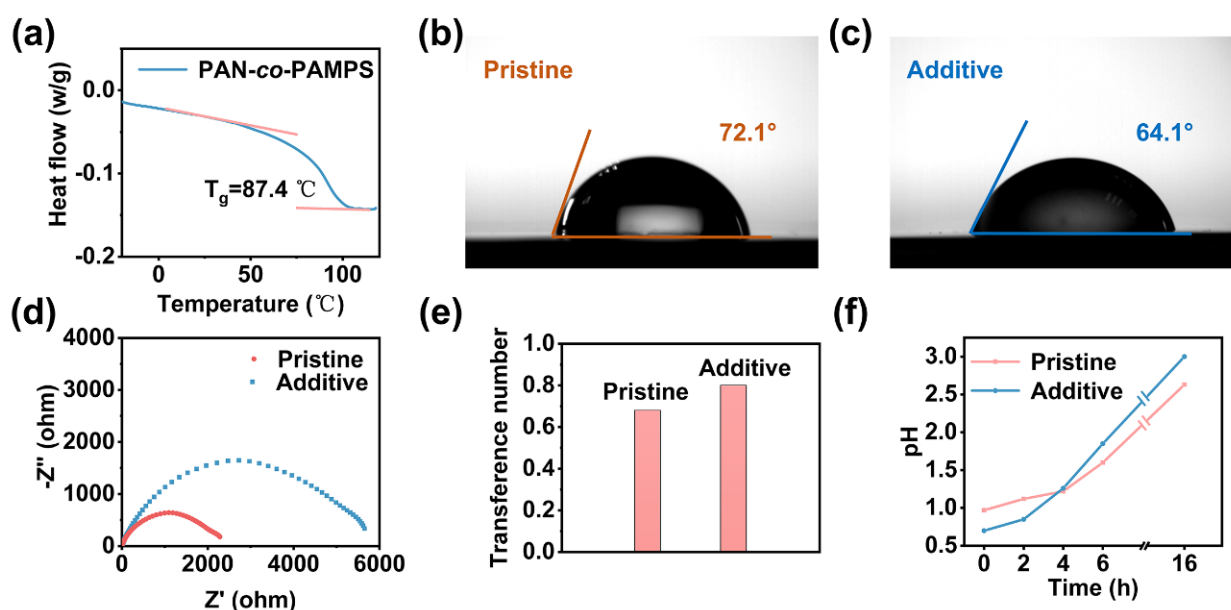


Figure 2. Physicochemical properties of electrolyte. (a) DSC of PAN-*co*-PAMPS. (b,c) Contact angles between pristine electrolyte and additive-containing electrolyte at 5 min. (d) Charge transfer resistance of Zn | Zn symmetric cell with pristine electrolyte and additive-containing electrolyte. (e) Transference number of Zn | Zn symmetric cells with pristine electrolyte and additive-containing electrolyte. (f) pH value changes of pristine and additive-containing electrolyte with soaked Zn metal.

The PAN-*co*-PAMPS copolymer containing 30 mol.% of AN and 70 mol.% of AMPS has several benefits when used as an electrolyte additive. Firstly, the hydrophilic PAMPS increases the compatibility electrolyte of the Zn electrode since PAMPS can react with Zn metal and then produce electrolyte polymer salts. Secondly, the lipophilic PAN provides a localized water-poor environment that resists the aqueous electrolyte contact with Zn metal. Thirdly, the acidic activation of the PAN-*co*-PAMPS copolymer can etch the zinc anode surface slightly, and strip oxides and other impurities from the zinc anode surface, but not destroy the zinc anode that benefits the plating. Though PAMPS is highly acidic, it reacts with the Zn anode very quickly, which does not destroy the Zn anode, but just strips the surface of the Zn anode and enhances the compatibility of the electrolyte and the zinc electrode. After 30 cycles, the contact angle between the additive-containing electrolyte and Zn is only 64.1°, which is lower than the 72.1° between the pristine electrolyte and Zn (Figure 2b,c). This indicates that the additive can increase the hydrophilicity of the Zn anode, which is beneficial to the uniform plating of zinc ions. Figures 2d and S5 show the charge transfer resistances of the Zn | Zn symmetric cell. The resistance of the Zn | Zn symmetric cell with an additive-containing electrolyte is 5133 Ω, which is higher than the control group of 1994 Ω. However, cells with an additive-containing electrolyte have a higher

transference number of 0.80 than cells with a pristine electrolyte of 0.68 (Figures 2e and S6). It may be caused by the additive stripping of the surface of the Zn anode. Higher ion migration capacity can deter the growth of Zn dendrites and prolong the life of the cell [38]. Figure 2f shows the pH value changes of pristine and additive-containing electrolytes after soaking the Zn metal for different time periods. The initial pH value of the pristine and additive-containing electrolyte was 0.97 and 0.70, respectively. The additive-containing electrolyte is much more acidic because of PAMPS. The sulfonic acid PAMPS can easily react with the impurities and oxides on the surface of Zn metal and yield salt. H^+ was consumed during the reaction, resulting in the increase of pH value. After etching with the Zn metal surface for 4 h, the pH value both increased and was kept basically equal. After 4 h, the pH value of the additive-containing electrolyte was higher than the pristine electrolyte. Figures 2f and S7 prove acidically reactive PAMPS can react with the Zn anode and peel the surface for better plating.

The Zn|Zn symmetric cells with additive-containing electrolytes can circulate for 2900 h at 1 mA cm^{-2} , which has an almost 10 times longer life than the cells with a pristine electrolyte (300 h) (Figure 3a). From inset of Figure 3a, we can see that the cell with a pristine electrolyte failed because of short circuiting. A possible reason for this may be because the additive peels on the Zn anode surface protects the Zn anode with a water-poor environment, and the zinc ions are deposited uniformly. The initial polarization voltage of the Zn|Zn symmetric cell using an additive-containing electrolyte is about 0.6 V, slightly higher than a cell with a pristine electrolyte (0.5 V), because of the additive increasing the interfacial resistance of the cell. The Zn|Zn symmetric cell with additive-containing electrolyte also shows excellent cycle life, circulating for 2400 h, which is 24 times longer than that with a pristine electrolyte (100 h) with the current density at 2 mA cm^{-2} (Figure 3b). Furthermore, the initial polarization voltage is also higher than a cell with a pristine electrolyte. A cell with a pristine electrolyte failed more quickly when the current density was 2 mA cm^{-2} than 1 mA cm^{-2} . This is because higher current density encourages the deposition of zinc ions and zinc ions is easier to deposit on the tip. Once the dendrites appear, they grow quickly, cross the separator, and then cause the short circuit. At a current density of 3 mA cm^{-2} , the Zn|Zn symmetric cell circulates for 900 h and then dies because of short circuiting (Figure 3c). As the current density increases, zinc dendrites can grow faster and easier. The current density changing from 0.2 mA cm^{-2} to 5 mA cm^{-2} and the rate performance of Zn|Zn symmetric cells is shown in Figure 3d. The Zn|Zn symmetric cell using an additive-containing electrolyte shows better regular symmetry and longer life than a cell with a pristine electrolyte at a different current density. This is attributed to the synergistic effect of PAN and PAMPS. PAMPS polishes the surface of the Zn anode first, and PAN forms on the water-poor surface.

The cell using an additive-containing electrolyte runs for 330 h under -20°C , which is much longer than the control group of 50 h (Figure 3e). The initial polarization voltage is about 0.3 V, higher than cell runs at room temperature, because the Zn ion transfers at a slower rate at a low temperature. The low temperature performance of the cell makes it possible for the cell with an additive to be used at a wider range of temperatures. Moreover, the Zn|Zn symmetric cell using an additive-containing electrolyte shows excellent performance at a high temperature up to 70°C with only 0.05 V initial polarization voltage, whereas the cell using a pristine electrolyte is dead before the temperature goes up to 60°C (Figure 3f). The thermostability of the polymer helps the additive to play the role, even at 70°C . The outstanding performance at a high temperature makes it have a wider application. A temperature increase is inevitable in many application scenarios, which launches a greater challenge for the high temperature performance of the cell.

Figure 4a,b show the SEM morphology of a Zn electrode with an additive-containing electrolyte and a pristine electrolyte at 1 mA cm^{-2} for 10, 30, 50 cycles, respectively. The surface of a Zn electrode with an additive-containing electrolyte is smooth with some etch, but the surface of a Zn anode with a pristine electrolyte is full of zinc dendrites. This is an intuitive description of the effect of the additive. PAMPS acts with Zn to remove

impurities and oxides on the surface, but does not destroy the Zn anode. The water-poor environment formed by PAN prevents dendrite growth. In contrast, the severe growth of dendrite on the surface of a cell with a pristine electrolyte may be the main cause of cell failure. Figure 4c further shows that cells with an additive-containing electrolyte produce less by-product during cycling. After cycling for 100 h, the peak of the by-product shown with a rhombus is much higher than cells with an additive-containing electrolyte. By-products lower the ion transport rate and consume more electrolytes, which reduce the life of the cell. Figure 4d,e shows the corrosion tendency of Zn|Zn cells. Figure 4d shows the Tafel curves of Zn with an additive-containing electrolyte and a pristine electrolyte. The corrosion potential of Zn with an additive-containing electrolyte is -0.009 V, higher than Zn with a pristine electrolyte (-0.014 V), with the corrosion current reducing from -2.212 mA cm $^{-2}$ to -2.858 mA cm $^{-2}$. This indicates that Zn with an additive-containing electrolyte tends to be much harder to corrode than Zn with a pristine electrolyte. Figure 4e shows the Chronoamperometry (CA) curves of Zn with an additive-containing electrolyte and a pristine electrolyte. For the cell with a pristine electrolyte, the current decreases hastily in 200 s, indicating that the zinc dendrites grow in two dimensions in the cell, which results in short circuiting. However, for the cell with an additive-containing electrolyte, the curve tends to be stable, which indicates 3D diffusion.

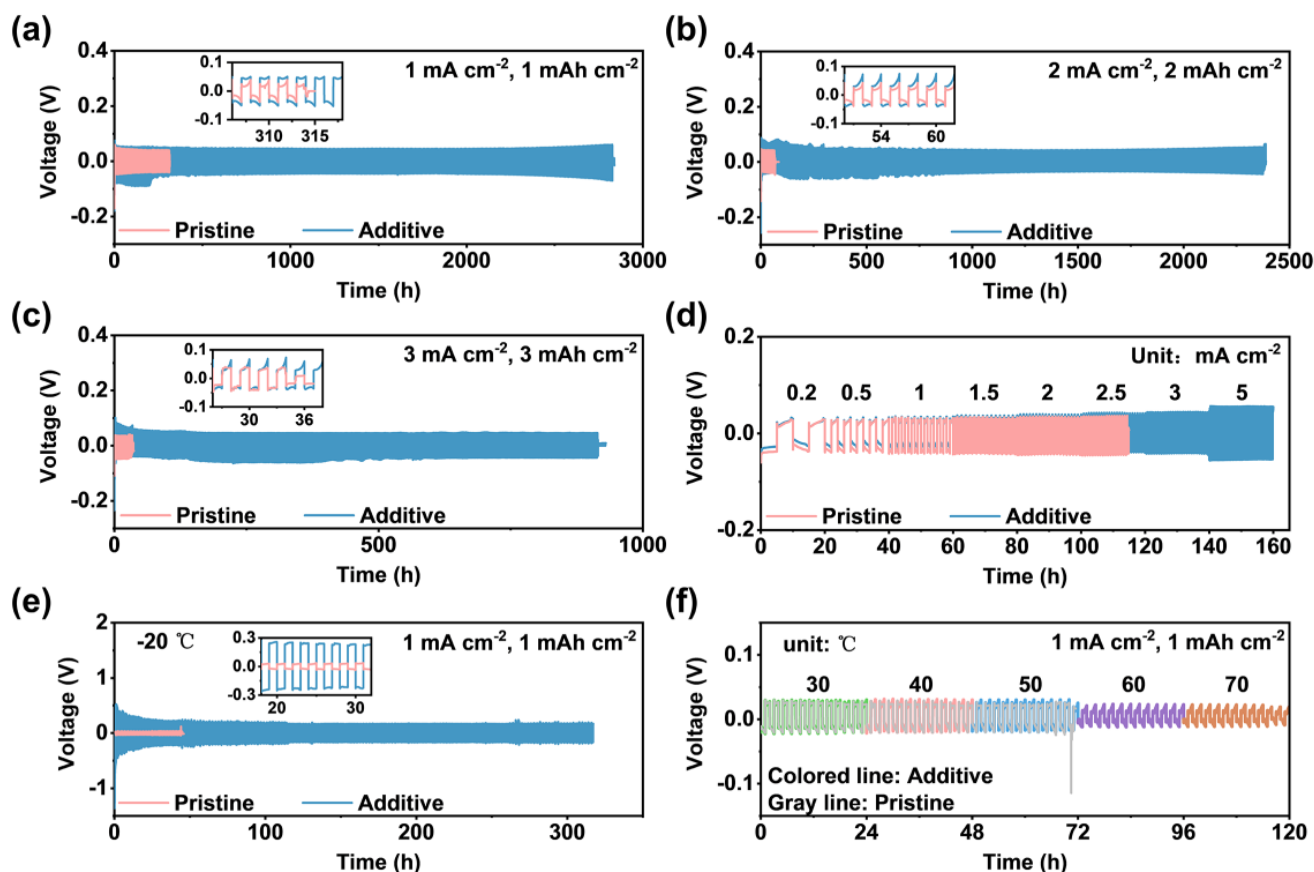


Figure 3. Electrochemical characteristics of Zn|Zn cells. (a–d) Zn|Zn symmetric cells with pristine electrolyte and additive-containing electrolyte at 1 mA cm $^{-2}$, 2 mA cm $^{-2}$, 3 mA cm $^{-2}$, and varying current densities. (e,f) Zn|Zn symmetric cells with pristine electrolyte and additive-containing electrolyte at -20 °C and different temperatures from 30 °C to 70 °C.

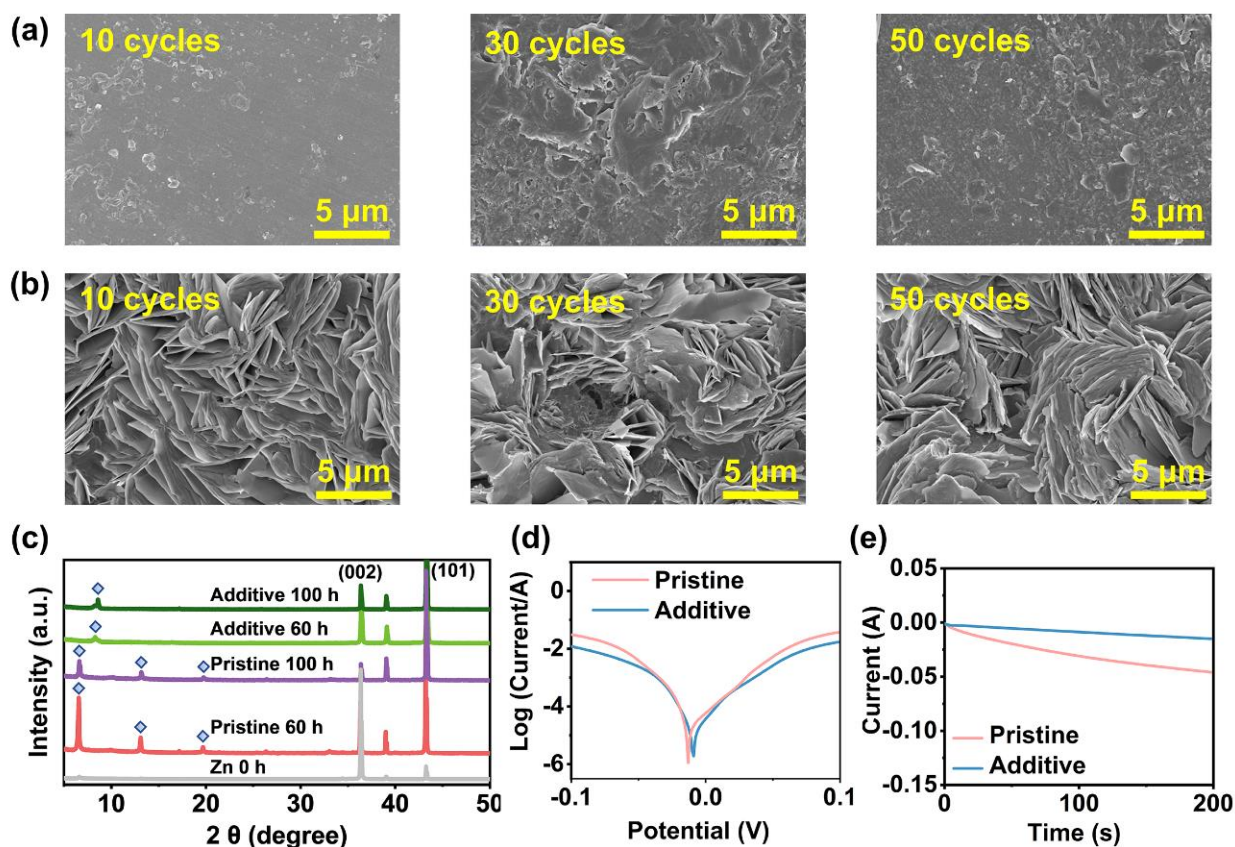


Figure 4. Plating condition of Zn^{2+} in $\text{Zn}|\text{Zn}$ cells. (a) Top-view SEM images of Zn anode obtained from $\text{Zn}|\text{Zn}$ cells with additive-containing electrolyte after cycling at 1 mA cm^{-2} . (b) Top-view SEM images of Zn anode obtained from $\text{Zn}|\text{Zn}$ cells with pristine electrolyte after cycling at 1 mA cm^{-2} . (c) XRD patterns of zinc surface from $\text{Zn}|\text{Zn}$ cells with additive-containing and pristine electrolyte after cycling at 1 mA cm^{-2} . (d) Tafel curves of Zn^{2+} with pristine and additive-containing electrolyte. (e) Tafel curves of $\text{Zn}|\text{Zn}$ cells with pristine and additive-containing electrolyte. Chronoamperograms (CAs) of $\text{Zn}|\text{Zn}$ cells with pristine and additive-containing electrolyte under a -10 mV overpotential.

The reversibility of Zn plating/stripping performance was performed by $\text{Zn}|\text{Cu}$ asymmetric cells. Figures 5a–c and S8 show the coulombic efficiency (CE) and voltage curve of $\text{Zn}|\text{Cu}$ asymmetric cells with a pristine electrolyte and an additive-containing electrolyte, respectively. Comparing the cells with a pristine electrolyte, cells with an additive-containing electrolyte present a higher CE when the current density is 1 mA cm^{-2} (99.3%), 2 mA cm^{-2} (99.6%), or 5 mA cm^{-2} (99.8%). Moreover, the voltage curves are all smooth. In addition to the cells with an additive-containing electrolyte, they live for more than 600 cycles at a current density of 1 mA cm^{-2} and 2 mA cm^{-2} current density. By contrast, the cells with an unsteady pristine electrolyte cycle, with a much lower CE and fluctuant voltage curve, fail after 100 cycles, which could result from side reactions such as dendrite growth. The much longer cycle life could be attributed to the lipophilic PAN providing a localized water-poor environment, which favors 3D diffusion.

$\text{Zn}|\text{V}_2\text{O}_5$ full batteries were also assembled to test the performance of an additive-containing electrolyte. Figures 5d,e and S9 show that, at a current density of 1 A g^{-1} , the $\text{Zn}|\text{V}_2\text{O}_5$ full batteries with an additive-containing electrolyte show the specific capacity of 341 mA h g^{-1} , maintaining a flat voltage platform on the charge–discharge curve, which is higher than batteries with a pristine electrolyte (260 mA h g^{-1}). Furthermore, batteries with an additive-containing electrolyte show a specific capacity of 190 mA h g^{-1} at 2 A g^{-1} , whereas the batteries with a pristine electrolyte only show a specific capacity of 70 mA h g^{-1} .

These results further confirm that PAN-co-PAMPS is a powerful modifier for electrolytes in zinc-ion batteries. Furthermore, with the additive, batteries show a more stable CE and maintain more than 400 cycles. The higher specific capacity could be caused by the additive restraining the formation of dendrite and water-related side reactions. In the initial several cycles, because of the activation of V_2O_5 , the capacity increases gradually. These results prove that the additive has a broad application prospect in the preparation of highly reversible energy storage devices.

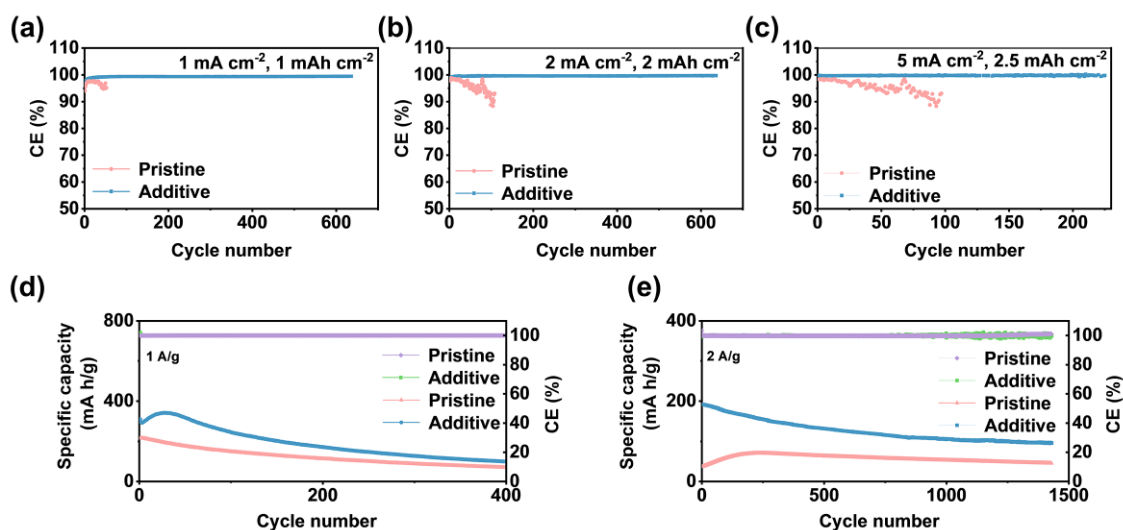


Figure 5. Electrochemical performance of Zn|Cu asymmetric cells and Zn|V₂O₅ full batteries. (a–c) Zn|Cu asymmetric cells using pristine electrolyte and additive-containing electrolyte when the current density is 1 mA cm⁻², 2 mA cm⁻², and 5 mA cm⁻². (d,e) Zn|V₂O₅ full batteries with pristine electrolyte and additive-containing electrolyte when the current density is 1 mA cm⁻² and 2 mA cm⁻².

3. Conclusions

The amphiphilic PAN-co-PAMPS polymer electrolyte additive with ionic and hydrophilicity PAMPS and non-ionic PAN demonstrates superior Zn-deposition capability in traditional aqueous Zn-ion batteries. The polymer can be well dissolved in an aqueous electrolyte solution while providing a localized hydrophobic environment at a molecular level to desolvate Zn²⁺ and shield the Zn anode from the attack of H₂O. The sulfonic acid units of the PAMPS chemically polish the surface of the Zn anode, leading to much reduced heterogeneity, which is beneficial to homogeneous Zn deposition. The hydrophobic PAN segments create a water-repelling effect that produces a less corrosive electrolyte environment, as evidenced by the increased oxygen evolution potential of the batteries assembled with polymer additive-containing Zn(CF₃SO₃)₂. As a result, the Zn|Zn symmetric cell containing a PAN-co-PAMPS additive delivers a long cycle life of more than 2900 h at 1 mA cm⁻² (1 mA h cm⁻²), which is about eight times longer than those without an additive. This work provides an easy-to-operate strategy for designing a multi-functional electrolyte additive and brings new insight into aqueous zinc storage devices.

Supplementary Materials: The following supporting information can be downloaded at: <https://www.mdpi.com/article/10.3390/batteries9010025/s1>, Figure S1: FTIR spectra of PAN and PAN-co-PAMPS; Figure S2: ¹H NMR spectrum of PAN-co-PAMPS molecule with peak assignments and integrals; Figure S3: Photographs of 1 M Zn(CF₃SO₃)₂ with 0, 0.5, 1 wt.% additive; Figure S4: Zn|Zn symmetric cells with pristine electrolyte, additive-containing electrolyte and 1wt.% additive electrolyte at a current density of 5 mA cm⁻²; Figure S5: Nyquist plots and fitted results of Zn|Zn symmetric cells with (a) Pristine electrolyte and (b) Additive-containing electrolyte. (c) Equivalent circuit used for EIS fitting, where R_s and R_{ct} represent ohmic resistance and polarization at Zn/electrolyte interface, respectively; Figure S6: Current-time curves of Zn|Zn symmetric cells with

(a) Pristine electrolyte and (b) Additive-containing electrolyte under a polarization voltage of 10 mV at room temperature. Inset: corresponding EIS curves before and after polarization; Figure S7: Photo of Zn metal. (a) Initial Zn metal. (b) Soaked in pristine electrolyte for 16 h. (c) Soaked in additive-containing electrolyte for 16 h; Figure S8: Voltage profiles of Zn | Cu asymmetric cells at selected cycles. (a) and (b) Zn | Cu asymmetric cells at a current density of 1 mA cm⁻², 1 mA cm⁻². (c) and (d) Zn | Cu asymmetric cells at a current density of 2 mA cm⁻², 2 mA cm⁻². (e) and (f) Zn | Cu asymmetric cells at a current density of 5 mA cm⁻², 2.5 mA cm⁻²; Figure S9: Galvanostatic capacity-voltage curves at 1 A g⁻¹ of Zn | V₂O₅ full batteries with (a) Pristine electrolyte and (b) Additive-containing electrolyte; Figure S10: A comparison chart of the cycling life versus current density and capacity for the device; Figure S11: EIS results after cycling for the cell; Figure S12: CV results for Zn | Zn symmetry cell with pristine and additive-containing electrolyte; Figure S13: Investigation of interfacial chemistry. XPS of Zn anode after cycling 24 h with additive-containing electrolyte at a current density of 1 mA cm⁻² with a capacity of 1 mA h cm⁻² obtained from (a) Zn | Zn symmetric cell and (b) Zn | V₂O₅ full battery; Table S1: Molecular weight and PDI of PAN-co-PAMPS; Table S2: Cycling performance of Zn | Zn symmetric cells with different additives [37–40].

Author Contributions: Conceptualization, X.W.; investigation, Y.-E.L.; resources, Y.-E.L.; software, Y.-E.L.; formal analysis, Y.-E.L.; original writing—review and editing, Y.-E.L. and X.W.; project administration, X.W.; funding acquisition, X.W. All authors have read and agreed to the published version of the manuscript.

Funding: Songshan Lake Materials Laboratory (Y1D1031H311).

Institutional Review Board Statement: Not applicable.

Informed Consent Statement: Not applicable.

Data Availability Statement: All collected data are presented in the manuscript.

Acknowledgments: Yu-E Liu acknowledges Jia Wang and Ben Niu for their help on image analysis and experimental instructions in this work.

Conflicts of Interest: The authors declare that they have no conflict of interest to report regarding the present study.

References

1. Gao, J.; Xie, X.; Liang, S.; Lu, B.; Zhou, J. Inorganic Colloidal Electrolyte for Highly Robust Zinc-Ion Batteries. *Nano-Micro Lett.* **2021**, *13*, 69. [[CrossRef](#)] [[PubMed](#)]
2. Nam, K.W.; Kim, H.; Beldjoudi, Y.; Kwon, T.-W.; Kim, D.J.; Stoddart, J.F. Redox-Active Phenanthrenequinone Triangles in Aqueous Rechargeable Zinc Batteries. *J. Am. Chem. Soc.* **2020**, *142*, 2541–2548. [[CrossRef](#)] [[PubMed](#)]
3. Wu, J.; Yuan, C.; Li, T.; Yuan, Z.; Zhang, H.; Li, X. Dendrite-Free Zinc-Based Battery with High Areal Capacity via the Region-Induced Deposition Effect of Turing Membrane. *J. Am. Chem. Soc.* **2021**, *143*, 13135–13144. [[CrossRef](#)] [[PubMed](#)]
4. Yan, L.; Zhang, Y.; Ni, Z.; Zhang, Y.; Xu, J.; Kong, T.; Huang, J.; Li, W.; Ma, J.; Wang, Y. Chemically Self-Charging Aqueous Zinc-Organic Battery. *J. Am. Chem. Soc.* **2021**, *143*, 15369–15377. [[CrossRef](#)]
5. Yang, W.; Du, X.; Zhao, J.; Chen, Z.; Li, J.; Xie, J.; Zhang, Y.; Cui, Z.; Kong, Q.; Zhao, Z.; et al. Hydrated Eutectic Electrolytes with Ligand-Oriented Solvation Shells for Long-Cycling Zinc-Organic Batteries. *Joule* **2020**, *4*, 1557–1574. [[CrossRef](#)]
6. Soundharajan, V.; Sambandam, B.; Kim, S.; Islam, S.; Jo, J.; Kim, S.; Mathew, V.; Sun, Y.-K.; Kim, J. The Dominant Role of Mn²⁺ Additive on the Electrochemical Reaction in ZnMn₂O₄ Cathode for Aqueous Zinc-ion Batteries. *Energy Storage Mater.* **2020**, *28*, 407–417. [[CrossRef](#)]
7. Ma, L.; Chen, S.; Li, N.; Liu, Z.; Tang, Z.; Zapien, J.A.; Chen, S.; Fan, J.; Zhi, C. Hydrogen-Free and Dendrite-Free All-Solid-State Zn-Ion Batteries. *Adv Mater.* **2020**, *32*, e1908121. [[CrossRef](#)]
8. Zuo, Y.; Wang, K.; Pei, P.; Wei, M.; Liu, X.; Xiao, Y.; Zhang, P. Zinc Dendrite Growth and Inhibition Strategies. *Mater. Today Energy* **2021**, *20*, 100692. [[CrossRef](#)]
9. Yi, Z.; Chen, G.; Hou, F.; Wang, L.; Liang, J. Strategies for the Stabilization of Zn Metal Anodes for Zn-Ion Batteries. *Adv. Energy Mater.* **2020**, *11*, 2003065. [[CrossRef](#)]
10. Liu, C.; Xie, X.; Lu, B.; Zhou, J.; Liang, S. Electrolyte Strategies toward Better Zinc-Ion Batteries. *ACS Energy Lett.* **2021**, *6*, 1015–1033. [[CrossRef](#)]
11. Javed, M.S.; Lei, H.; Wang, Z.; Liu, B.-T.; Cai, X.; Mai, W. 2D V₂O₅ Nanosheets as a Binder-free High-energy Cathode for Ultrafast Aqueous and Flexible Zn-ion Batteries. *Nano Energy* **2020**, *70*, 104573. [[CrossRef](#)]

12. Javed, M.S.; Shah, S.S.A.; Najam, T.; Siyal, S.H.; Hussain, S.; Saleem, M.; Zhao, Z.; Mai, W. Achieving High-energy Density and Superior Cyclic Stability in Flexible and Lightweight Pseudocapacitor through Synergic Effects of Binder-free CoGa_2O_4 2D-hexagonal Nanoplates. *Nano Energy* **2020**, *77*, 105276. [[CrossRef](#)]
13. Javed, M.S.; Shaheen, N.; Hussain, S.; Li, J.; Shah, S.S.A.; Abbas, Y.; Ahmad, M.A.; Raza, R.; Mai, W. An Ultra-high Energy Density Flexible Asymmetric Supercapacitor Based on Hierarchical Fabric Decorated with 2D Bimetallic Oxide Nanosheets and MOF-derived Porous Carbon Polyhedra. *J. Mater. Chem. A* **2019**, *7*, 946–957. [[CrossRef](#)]
14. Javed, M.S.; Mateen, A.; Ali, S.; Zhang, X.; Hussain, I.; Imran, M.; Shah, S.S.A.; Han, W. The Emergence of 2D MXenes Based Zn-Ion Batteries: Recent Development and Prospects. *Small* **2022**, *18*, 2201989. [[CrossRef](#)] [[PubMed](#)]
15. Wang, D.; Li, Q.; Zhao, Y.; Hong, H.; Li, H.; Huang, Z.; Liang, G.; Yang, Q.; Zhi, C. Insight on Organic Molecules in Aqueous Zn-Ion Batteries with an Emphasis on the Zn Anode Regulation. *Adv. Energy Mater.* **2022**, *12*, 2102707. [[CrossRef](#)]
16. Guo, S.; Qin, L.; Zhang, T.; Zhou, M.; Zhou, J.; Fang, G.; Liang, S. Fundamentals and Perspectives of Electrolyte Additives for Aqueous Zinc-ion Batteries. *Energy Storage Mater.* **2021**, *34*, 545–562. [[CrossRef](#)]
17. Sun, P.; Ma, L.; Zhou, W.; Qiu, M.; Wang, Z.; Chao, D.; Mai, W. Simultaneous Regulation on Solvation Shell and Electrode Interface for Dendrite-Free Zn Ion Batteries Achieved by a Low-Cost Glucose Additive. *Angew. Chem. Int. Ed.* **2021**, *60*, 18247–18255. [[CrossRef](#)]
18. Qin, R.; Wang, Y.; Zhang, M.; Wang, Y.; Ding, S.; Song, A.; Yi, H.; Yang, L.; Song, Y.; Cui, Y.; et al. Tuning Zn^{2+} Coordination Environment to Suppress Dendrite Formation for High-performance Zn-ion Batteries. *Nano Energy* **2021**, *80*, 105478. [[CrossRef](#)]
19. Zhao, J.; Zhang, J.; Yang, W.; Chen, B.; Zhao, Z.; Qiu, H.; Dong, S.; Zhou, X.; Cui, G.; Chen, L. “Water-in-deep Eutectic Solvent” Electrolytes Enable Zinc Metal Anodes for Rechargeable Aqueous Batteries. *Nano Energy* **2019**, *57*, 625–634. [[CrossRef](#)]
20. Cao, L.; Li, D.; Hu, E.; Xu, J.; Deng, T.; Ma, L.; Wang, Y.; Yang, X.-Q.; Wang, C. Solvation Structure Design for Aqueous Zn Metal Batteries. *J. Am. Chem. Soc.* **2020**, *142*, 21404–21409. [[CrossRef](#)]
21. Hosseini, S.; Abbasi, A.; Uginet, L.-O.; Haustraete, N.; Praserthdam, S.; Yonezawa, T.; Kheawhom, S. The Influence of Dimethyl Sulfoxide as Electrolyte Additive on Anodic Dissolution of Alkaline Zinc-Air Flow Battery. *Sci. Rep.* **2019**, *9*, 14958. [[CrossRef](#)] [[PubMed](#)]
22. Kao-Ian, W.; Nguyen, M.T.; Yonezawa, T.; Pornprasertsuk, R.; Qin, J.; Siwamogsatham, S.; Kheawhom, S. Highly Stable Rechargeable Zinc-ion Battery using Dimethyl Sulfoxide Electrolyte. *Mater. Today Energy* **2021**, *21*, 100738. [[CrossRef](#)]
23. Kaveevivitchai, W.; Manthiram, A. High-capacity Zinc-ion Storage in an Open-tunnel Oxide for Aqueous and Nonaqueous Zn-ion Batteries. *J. Mater. Chem. A* **2016**, *4*, 18737–18741. [[CrossRef](#)]
24. Hou, Z.; Tan, H.; Gao, Y.; Li, M.; Lu, Z.; Zhang, B. Tailoring Desolvation Kinetics Enables Stable Zinc Metal Anodes. *J. Mater. Chem. A* **2020**, *8*, 19367–19374. [[CrossRef](#)]
25. Song, X.; He, H.; Shiraz, M.H.A.; Zhu, H.; Khosrozadeh, A.; Liu, J. Enhanced Reversibility and Electrochemical Window of Zn-ion Batteries with an Acetonitrile/water-in-salt Electrolyte. *Chem. Commun.* **2021**, *57*, 1246–1249. [[CrossRef](#)] [[PubMed](#)]
26. Song, Y.; Tang, J.; Hu, J.; Yang, H.; Gu, W.; Fu, Y.; Ji, X. Interfacial Assistant Role of Amine Additives on Zinc Electrodeposition from Deep Eutectic Solvents: An in situ X-ray Imaging Investigation. *Electrochim. Acta* **2017**, *240*, 90–97. [[CrossRef](#)]
27. Liu, S.; Mao, J.; Pang, W.K.; Vongsvivut, J.; Zeng, X.; Thomsen, L.; Wang, Y.; Liu, J.; Li, D.; Guo, Z. Tuning the Electrolyte Solvation Structure to Suppress Cathode Dissolution, Water Reactivity, and Zn Dendrite Growth in Zinc-Ion Batteries. *Adv. Funct. Mater.* **2021**, *31*, 2104281. [[CrossRef](#)]
28. Naveed, A.; Yang, H.; Shao, Y.; Yang, J.; Yanna, N.; Liu, J.; Shi, S.; Zhang, L.; Ye, A.; He, B.; et al. A Highly Reversible Zn Anode with Intrinsically Safe Organic Electrolyte for Long-Cycle-Life Batteries. *Adv. Mater.* **2019**, *31*, 1900668. [[CrossRef](#)]
29. Feng, R.; Chi, X.; Qiu, Q.; Wu, J.; Huang, J.; Liu, J.; Liu, Y. Cyclic Ether–Water Hybrid Electrolyte-Guided Dendrite-Free Lamellar Zinc Deposition by Tuning the Solvation Structure for High-Performance Aqueous Zinc-Ion Batteries. *ACS Appl. Mater. Interfaces* **2021**, *13*, 40638–40647. [[CrossRef](#)]
30. Abdulla, J.; Cao, J.; Zhang, D.; Zhang, X.; Sriprachubwong, C.; Kheawhom, S.; Wangyao, P.; Qin, J. Elimination of Zinc Dendrites by Graphene Oxide Electrolyte Additive for Zinc-Ion Batteries. *ACS Appl. Energy Mater.* **2021**, *4*, 4602–4609. [[CrossRef](#)]
31. Wang, F.; Borodin, O.; Gao, T.; Fan, X.; Sun, W.; Han, F.; Faraone, A.; Dura, J.A.; Xu, K.; Wang, C. Highly Reversible Zinc Metal Anode for Aqueous Batteries. *Nat. Mater.* **2018**, *17*, 543–549. [[CrossRef](#)] [[PubMed](#)]
32. Zhang, C.; Shin, W.; Zhu, L.; Chen, C.; Neuefeind, J.C.; Xu, Y.; Allec, S.I.; Liu, C.; Wei, Z.; Daniyar, A.; et al. The Electrolyte comprising More Robust Water and Superhalides Transforms Zn-metal Anode Reversibly and Dendrite-free. *Carbon Energy* **2020**, *3*, 339–348. [[CrossRef](#)]
33. Yang, J.; Zhang, Y.; Li, Z.; Xu, X.; Su, X.; Lai, J.; Liu, Y.; Ding, K.; Chen, L.; Cai, Y.; et al. Three Birds with One Stone: Tetramethylurea as Electrolyte Additive for Highly Reversible Zn-Metal Anode. *Adv. Funct. Mater.* **2022**, *32*, 2209642. [[CrossRef](#)]
34. Qin, H.; Kuang, W.; Hu, N.; Zhong, X.; Huang, D.; Shen, F.; Wei, Z.; Huang, Y.; Xu, J.; He, H. Building Metal-Molecule Interface towards Stable and Reversible Zn Metal Anodes for Aqueous Rechargeable Zinc Batteries. *Adv. Funct. Mater.* **2022**, *32*, 2206695. [[CrossRef](#)]
35. Gao, H.; Lian, K. Proton-conducting Polymer Electrolytes and Their Applications in Solid Supercapacitors: A review. *RSC Adv.* **2014**, *4*, 33091–33113. [[CrossRef](#)]
36. Afrifah, V.A.; Phiri, I.; Hamenu, L.; Madzvamuse, A.; Lee, K.S.; Ko, J.M. Electrochemical Properties of Poly(2-acrylamido-2-methylpropane sulfonic acid) Polyelectrolyte Containing Zwitterionic Silica Sulfobetaine for Supercapacitors. *J. Power Sources* **2020**, *479*, 228657. [[CrossRef](#)]

37. Niu, B.; Li, Z.; Cai, S.; Luo, D.; Qiao, Y.; Zhou, S.; Li, H.; He, X.; Wang, X. Robust Zn Anode Enabled by a Hydrophilic Adhesive Coating for Long-life Zinc-ion Hybrid Supercapacitors. *Chem. Eng. J.* **2022**, *442*, 136217. [[CrossRef](#)]
38. Zhou, H.; Li, M.; Zhu, J.; Chen, R.; Wang, X.; Wang, H.-L. Exploring Polymer Precursors for Low-cost High Performance Carbon fiber: A Materials Genome Approach to Finding Polyacrylonitrile-co-poly(N-vinyl formamide). *Polymer* **2022**, *243*, 124570. [[CrossRef](#)]
39. Liu, H.; Zhang, S.; Yang, J.; Ji, M.; Yu, J.; Wang, M.; Chai, X.; Yang, B.; Zhu, C.; Xu, J. Preparation, Stabilization and Carbonization of a Novel Polyacrylonitrile-Based Carbon Fiber Precursor. *Polymers* **2019**, *11*, 1150. [[CrossRef](#)]
40. Liu, H.; Luo, Q.; Zhang, S.; Shi, L.; Yang, J.; Liu, R.; Wang, M.; Zhu, C.; Xu, J. New Comonomer for Polyacrylonitrile-based Carbon Fiber: Density Functional Theory Study and Experimental Analysis. *Polymer* **2018**, *153*, 369–377. [[CrossRef](#)]

Disclaimer/Publisher's Note: The statements, opinions and data contained in all publications are solely those of the individual author(s) and contributor(s) and not of MDPI and/or the editor(s). MDPI and/or the editor(s) disclaim responsibility for any injury to people or property resulting from any ideas, methods, instructions or products referred to in the content.